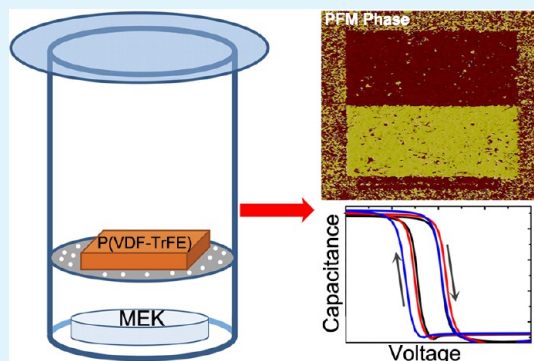


# Solvent Vapor Annealing of Ferroelectric P(VDF-TrFE) Thin Films

Jinghang Hu,<sup>†</sup> Jianchi Zhang,<sup>‡</sup> Zongyuan Fu,<sup>†</sup> Yulong Jiang,<sup>‡</sup> Shijin Ding,<sup>\*,‡</sup> and Guodong Zhu<sup>\*,†</sup><sup>†</sup>Department of Materials Science, Fudan University, Shanghai 200433, China<sup>‡</sup>School Microelectronics, Fudan University, Shanghai 200433, China

**ABSTRACT:** Ferroelectric polymers are a kind of promising materials for low-cost flexible memories. However, the relatively high thermal annealing temperature restricts the selection of some flexible polymer substrates. Here we report an alternative method to obtain ferroelectric poly(vinylidene fluoride-co-trifluoroethylene) (P(VDF-TrFE)) thin films under low process temperatures. Spin-coated P(VDF-TrFE) thin films were solvent vapor processed at 30 °C for varied times. Structural analyses indicated that solvent vapor annealing induced crystallization to form a ferroelectric  $\beta$  phase, and electrical measurements from both macroscopic ferroelectric switching and microscopic vertical piezoresponse force microscopy further proved the films enduring solvent vapor annealing for suitable short times possessed good ferroelectric and piezoelectric properties. To illuminate the application of solvent vapor annealing on ferroelectric devices, we further fabricated ferroelectric capacitor memory devices with a structure of Al/P(VDF-TrFE)/Al<sub>2</sub>O<sub>3</sub>/p-Si/Al where the ferroelectric layer was solvent vapor annealed. Ferroelectric capacitors showed obvious bistable operation and comparable ON/OFF ratio and retention performance. Our work makes it possible to structure ferroelectric devices on flexible substrates that require low process temperatures.

**KEYWORDS:** ferroelectric polymer, solvent vapor annealing, P(VDF-TrFE)



## INTRODUCTION

The field of organic electronics has attracted increased attention due to its potential for large-area electronic applications such as flexible displays and smart labels. Organic transistors and displays have entered the market; however, organic nonvolatile memories are still the main bottleneck that narrows the applications of all-organic flexible electronic systems.<sup>1</sup> Among all reported organic nonvolatile memories, organic ferroelectric memories have been comprehensively studied and regarded as a promising technology for low-cost flexible memories. Ferroelectric polymers, especially poly(vinylidene fluoride-co-trifluoroethylene) (P(VDF-TrFE)), and organic semiconductors, such as pentacene and poly(3-hexylthiophene-2,5-diyl) (P3HT), are integrated to form ferroelectric field-effect transistors (OFETs) for nonvolatile memory function.<sup>2</sup>

Ferroelectric polymer films are mostly semicrystalline with coexistence of amorphous and crystalline phases. To improve their degree of crystallinity and thus enhance their ferroelectric properties, it is required to thermally anneal spin-coated P(VDF-TrFE) films at a temperature between their glass transition and melting temperature.<sup>3</sup> This high annealing temperature, usually between 130 and 145 °C,<sup>3</sup> may exceed the temperature limit that some flexible polymer substrates can endure or dissatisfy the temperature requirement during the device fabrication process, thus resulting in restricted application of ferroelectric polymer films on flexible devices. It is much attractive to develop a solution for low-temperature

enhancement of crystallinity and ferroelectricity in ferroelectric polymer films.

One promising way to increase the molecular ordering and film crystallinity at low temperatures is by exposing the organic films to an environment filled with a specific solvent vapor, referred to as solvent vapor annealing (SVA).<sup>4</sup> A solvent vapor diffuses into the deposited organic layer, the extent of which is dependent on and thus controlled by exposure time and even the solvent polarity,<sup>5</sup> swells the organic layer and enables the formation of a “soft phase”, which causes an increase in polymer-chain mobility similar to thermal annealing and allows the molecules to reorganize with a higher degree of freedom than in a solid phase and drives the system to evolve toward a more thermodynamically stable morphology. SVA can be done at room temperature, significantly reducing the risk of thermal degradation of the material, and has been increasingly regarded as an appealing option for the self-assembly of ordered nanostructures in block polymer films,<sup>6,7</sup> the fabrication of micro/nanoscaled particles and wires in organic semiconductors<sup>8,9</sup> and the enhancement of device performance in organic thin film transistors<sup>4,10</sup> and organic solar cells.<sup>11,12</sup> Here we report our recent work on solvent vapor annealing of ferroelectric polymer films.

Received: August 19, 2014

Accepted: September 22, 2014

Published: September 22, 2014

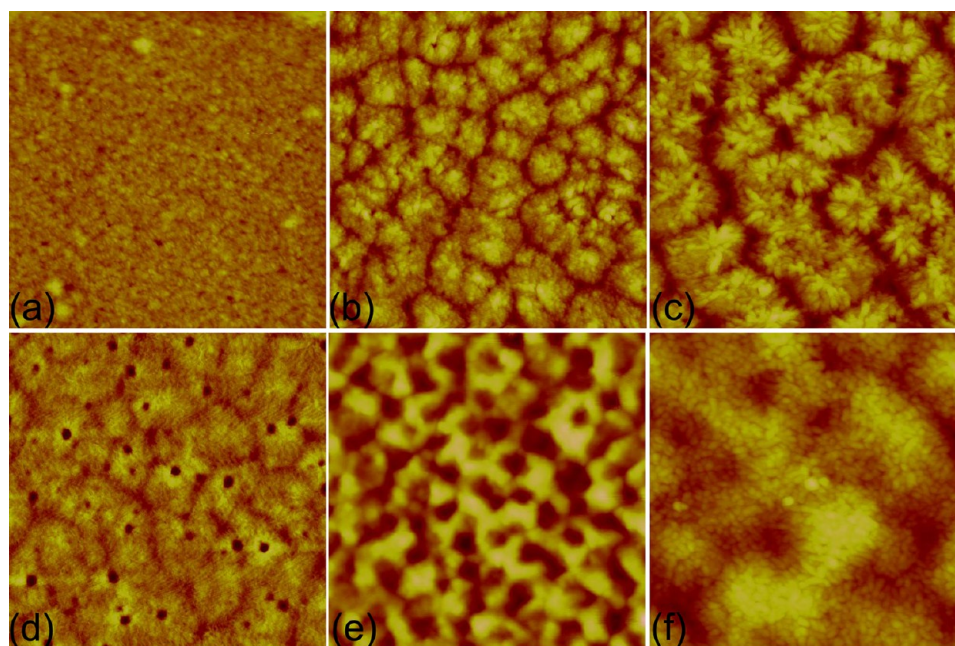


**Figure 1.** AFM morphologies of (a) as-cast, (b–e) solvent vapor and (f) thermally annealed P(VDF-TrFE) films. For the samples in panels b–e, the films were solvent vapor annealed at 30 °C for 4, 6, 8 and 16 h, respectively, whereas the sample in panel f was thermally annealed at 135 °C for 3 h. AFM was operated at tapping mode with probe resonance frequency of 175 kHz.

## RESULTS AND DISCUSSION

P(VDF-TrFE) thin films were spin-coated from a 1.0% by weight solution of 60/40 P(VDF-TrFE) in methyl ethyl ketone (MEK). These as-cast films were put into a sealed glass container filled with about 15 mL of MEK solvent at 30 °C for a preset time. The typical morphologies of these SVA-treated P(VDF-TrFE) films are characterized by atomic force microscopy (AFM) and are shown in Figure 1. The as-coated film shows a smooth surface with a root-mean-square (RMS) roughness of 1.68 nm (Figure 1a); with the increase of SVA time to 6 h, large aggregations with diameter of several hundred nanometers appears on the film surface (Figure 1b) and then smaller crystalline grains grow out of these large aggregations (Figure 1c); the crystallization process also increases RMS roughness to 4.24 and 7.36 nm for the samples in panels b and c, respectively. With further increase of SVA time, MEK vapor corrodes P(VDF-TrFE) films, leaving small holes on the film surface (Figure 1d) and even damaging the integrality of the whole film with an even longer SVA time of 16 h (Figure 1e). For comparison, the morphology of thermally annealed P(VDF-TrFE) films is shown in Figure 1f, which also shows small crystalline grains, similar to that of the film SVA treated for 6 h in Figure 1c. Obviously, SVA treated P(VDF-TrFE) films show the same morphology evolution as thermally annealed films. Furthermore, here we focus on the low-temperature fabrication of ferroelectric thin films suitable for the applications in organic ferroelectric devices, which requires solid films with less defects and thus lower leakage current. A SVA time longer than 8 h induces holes and even results in discrete surfaces, unsatisfactory for our requirements. So, in the following work, we only pay attention to those films treated by relatively shorter SVA times, such as 4–6 h.

Though, from a comparison between the morphologies obtained from SVA and thermally treated films, we observe the similar small grains that almost cover the whole film surface and regard these small grains as crystalline ones; the next step is to

further determine phase and structural information by X-ray diffraction (XRD) analyses. In Figure 2 are shown the XRD

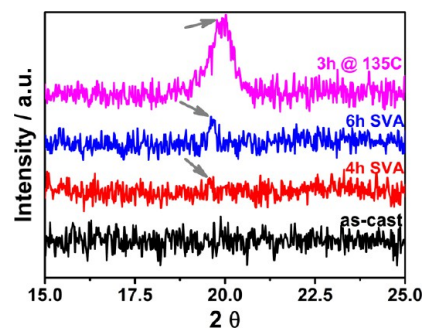


**Figure 2.** XRD analyses of as-cast, thermally annealed and SVA-treated P(VDF-TrFE) films. SVA treatment was done at 30 °C for 4 and 6 h, and the thermally annealed film was treated at 135 °C for 3 h.

spectra from as-cast, thermally annealed and SVA-treated P(VDF-TrFE) films. The as-cast film shows neglectable crystalline characteristic, whereas, after thermal annealing at 135 °C for 3 h, one crystalline peak at  $2\theta = 19.86^\circ$  occurs that comes from the superimposition of (200) and (110) reflections, indicating the existence of a crystalline  $\beta$ -polar phase in the P(VDF-TrFE) film.<sup>3</sup> As for the film exposed to MEK vapor for 4 h, though the spectrum is very noisy, we can still observe a contour of a characteristic peak at  $2\theta = 19.6^\circ$ , indicating the occurrence of crystalline  $\beta$ -polar phase after solvent vapor annealing. With further increase of exposure time, such as up to 6 h, this characteristic peak is further enhanced, indicating the improvement of crystallinity. Note that the crystalline peaks from SVA-treated films are much weaker than that from thermally annealed film. This is mainly due to the limited penetration of the MEK solvent into P(VDF-TrFE) film, which confines the thickening of crystalline layer. The enhancement of crystalline peaks with an increased SVA time from 4 to 6 h

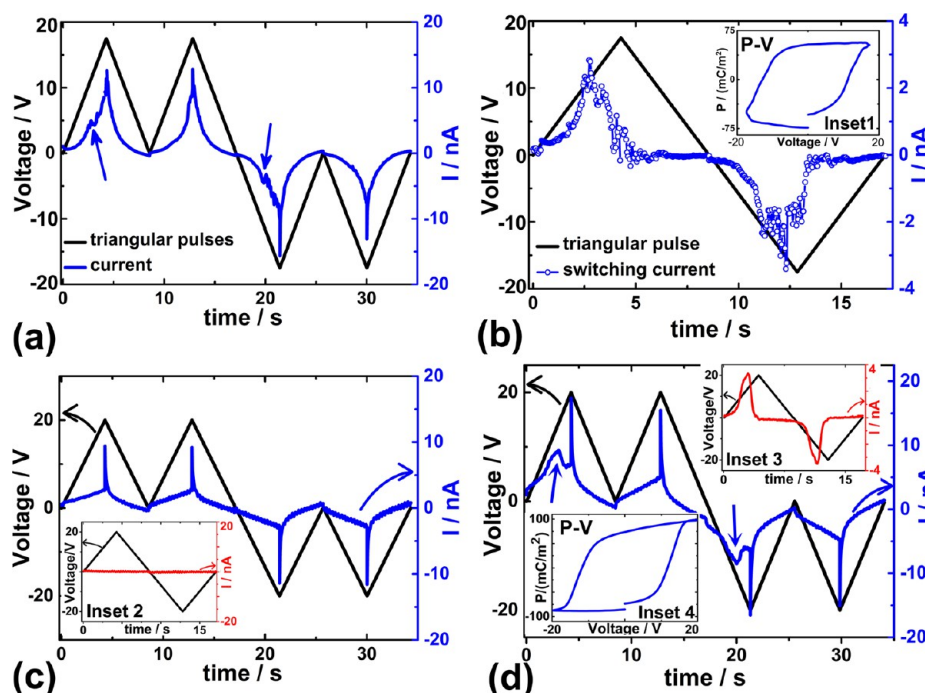


**Figure 3.** Ferroelectric switching measurements of a Al/P(VDF-TrFE)/Al structure. The P(VDF-TrFE) films were (a) solvent vapor annealed with exposure time of 6 h, (b) as-coated and (c) thermally annealed 135 °C for 3 h. Blue arrows in panels a and d indicate the positions of ferroelectric switching peaks. Insets 2 and 3 show the calculated switching current responses of as-coated and thermally annealed films, respectively, and insets 1 and 4 show the  $P$ - $V$  hysteresis loops of as-coated and thermally annealed films, which were obtained by integrating the switching current responses with time.

further proves that a longer exposure time is of great help for MEK vapor to diffuse deeper into the film and thus results in the formation of a thicker crystalline layer.

Solvent vapor annealing is based on positioning the as-cast films in an environment saturated with solvent vapor. The resulting reorganization of the functional materials at the surfaces is due to partial resolubilization of the as-cast film, allowing the molecules to rearrange into ordered structures. So, the depth that the solvent vapor can penetrate into the film will determine the thickness of the crystalline layer. It is postulated that during solvent vapor annealing, the solvent condenses on film surface, forming a continuous solvent layer with a thickness of a few nanometers,<sup>13</sup> which can be described as a quasi-two-dimensional solution.<sup>14</sup> With the increase of SVA time, the solvent may diffuse deeper into the film, resulting in thickening of the crystalline layer.

Through the AFM and XRD measurements, we have shown that solvent vapor annealing is effective to induce crystallization in P(VDF-TrFE) films at low temperatures. Electrical measurements were further performed to show that these SVA-treated P(VDF-TrFE) films do possess a ferroelectric property. Measurement of the ferroelectric property was performed with a homemade Sawyer-Tower circuit. The response of a ferroelectric material to a time-dependent applied voltage can be simply expressed by

$$I(t) = \frac{CdV(t)}{dt} + \frac{AdP(t)}{dt} + \sigma V(t) \quad (1)$$

where  $t$  and  $I$  are the time and the current, respectively,  $V(t)$  is time dependent applied voltage,  $C$  the capacitance of the ferroelectric film,  $A$  the effective electrode area,  $P(t)$  the time dependent polarization and  $\sigma$  the conductivity of the ferroelectric film. The first term in the right side of eq 1

stands for the dielectric displacement current of the film. The second term is the current due to ferroelectric switching, which is going to be extracted from the current–voltage measurements below. The third term is a superposition of linear conduction obeying the Ohm's Law<sup>15</sup> and ionic conduction caused by the impurities and defects in the films.<sup>16</sup> In the measurements of the ferroelectric property in our 150 nm thick P(VDF-TrFE) films, a large leakage current usually blurs the observation of the ferroelectric switching current, which is the third term in eq 1 and is comparable to or even larger than the second term. To the full extent of reducing the influence of dielectric and conduction currents, we applied sweep voltage combined with unipolar and bipolar pulses to the ferroelectric films, so-called “unipolar and bipolar voltage sweep”,<sup>15,17</sup> the waveform of which is shown in Figure 3a. The representative results are shown in Figure 3, where ferroelectric films were solvent vapor annealed at 30 °C for 6 h (Figure 3a,b), as-coated (Figure 3c) and thermally annealed at 135 °C for 3 h (Figure 3d), respectively. Before the application of the combined pulses, the ferroelectric film was first negatively prepolared by  $-20$  V voltage for 10 s. Then, as for the SVA-treated film in Figure 3a,b, two positive triangular pulses with an amplitude of 17.5 V and period of 8.5 s were sequentially applied. During the application of the first triangular pulse, the recorded current responses include all contributions from those three terms in eq 1; after the film has been poled by the first pulse, during the second triangular pulse, the recorded current responses should be attributed only to the dielectric displacement current (the first term in eq 1) and conduction current (the third term). Therefore, the neat switching current responses can be obtained from the difference between both current responses. When the two negative triangular pulses were applied, the same process occurred as what positive pulses did. Figure 3a shows



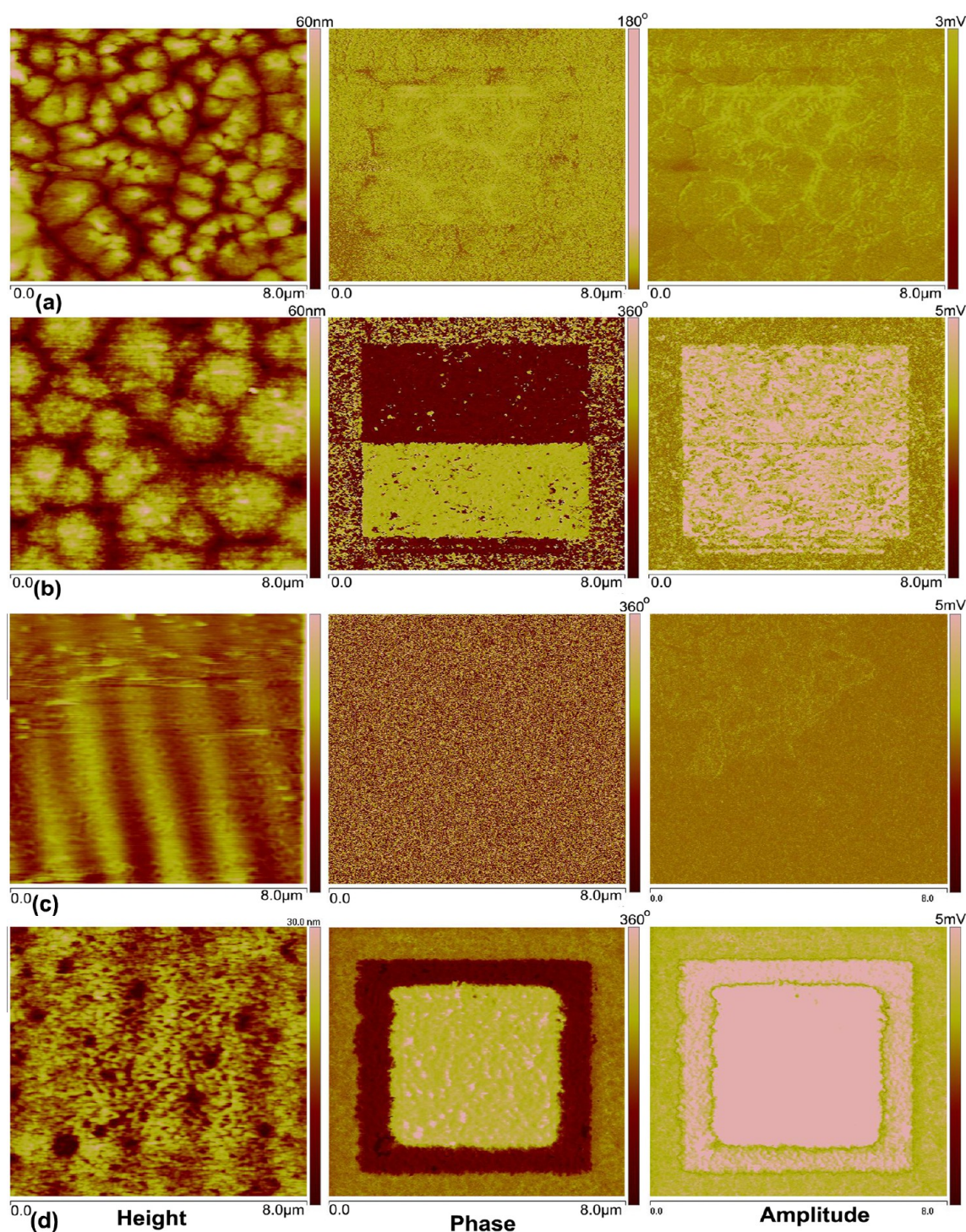


**Figure 4.** VPFM measurements of P(VDF-TrFE) films. The samples in panel sets a and b were solvent vapor annealed at 30 °C for 4 and 6 h and the samples in panel sets c and d were as-coated and thermally annealed at 135 °C for 3 h, respectively. From left to right are shown the height, VPFM phase and VPFM amplitude images. P(VDF-TrFE) films were spin-coated on glass slides predeposited with Al bottom electrodes.

the recorded current responses during the application of the combined pulses, and Figure 3b shows the neat switching current responses, which were obtained by subtracting the second current response from the first one. Due to the incomplete removal of leakage current, the switching current curve still includes the influence of leakage current. However, the switching current peaks shown in Figure 3b still undoubtedly prove the existence of ferroelectricity in SVA-treated P(VDF-TrFE) films. Integrating the switching current

responses with time, we got polarization–voltage ( $P$ – $V$ ) hysteresis loop (inset 1 in Figure 3b), which shows an averaged remanent polarization ( $P_r$ ) of 63.8 mC/m<sup>2</sup>. Note that this  $P_r$  value is not accurate because of the superimposition of some leakage current, and the unclosed loop indicates an asymmetric leakage current during the application of positive and negative pulses.

To further verify the reliability of our homemade Sawyer–Tower circuit for ferroelectric measurements, we also

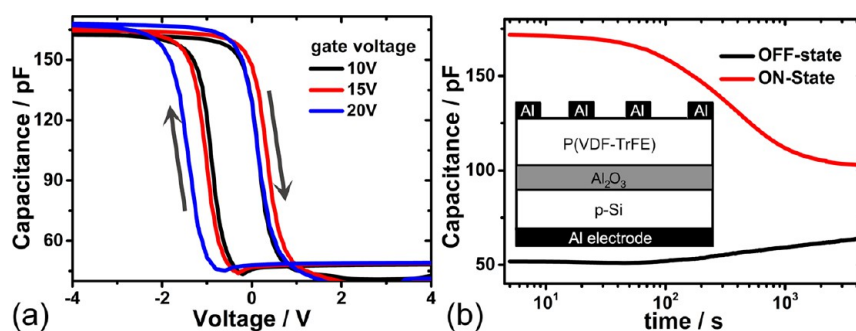


**Figure 5.** Capacitance measurements of Al/P(VDF-TrFE)/Al<sub>2</sub>O<sub>3</sub>/p-Si/Al structure. P(VDF-TrFE) layers were solvent vapor annealed at 30 °C for 6 h. (a)  $C$ - $V$  loops at various gate voltages. Arrows indicate the direction of voltage sweep. (b) Retention measurements of both ON- and OFF-states. Before retention measurements, a +20 V (−20 V) gate voltage was applied for 10 s to drive the ferroelectric memory device into OFF (ON) state and then retention was characterized at zero gate voltage. Inset shows the structure of the ferroelectric capacitors.

characterized the ferroelectric properties of as-coated and thermally annealed P(VDF-TrFE) films, shown in Figures 3c,d, respectively. As for the as-coated film, the first and second positive (negative) pulses induce nearly the same current responses and, after the subtraction of the second current response from the first one, we only get featureless and nearly zero switching current curve shown as inset 2 in Figure 3c, indicating the negligible ferroelectricity in as-coated P(VDF-TrFE) film. As for the thermally annealed film, obvious switching peaks, indicated by blue arrows in Figure 3d, occur during the application of the first positive (negative) pulses and the calculated switching current curve and  $P$ - $V$  hysteresis loop are shown as insets 3 and 4 in Figure 3d. The thermally annealed film shows an averaged remanent polarization of 78.5 mC/m<sup>2</sup>, slightly larger than that of SVA-treated film. These experimental results from as-coated and thermally annealed films are consistent with the well accepted understanding of ferroelectric P(VDF-TrFE) films and thus prove the reliability of our homemade Sawyer-Tower circuit for ferroelectric measurements.

Macroscopic ferroelectric switching measurements shown in Figure 3a,b have proved that by solvent vapor annealing at low temperature it is possible to obtain P(VDF-TrFE) films with a ferroelectric property. However, due to the influence of leakage current, the observed ferroelectric switching peaks and  $P$ - $V$  loop are not well characterized. To further characterize the electrical properties, we performed vertical piezoresponse force microscopy (VPFM) measurements on the P(VDF-TrFE)/Al structure. During all VPFM measurements, the conductive probe was electrically grounded and the applied voltage was applied to the bottom Al electrodes. VPFM was operated in contact mode with a driving amplitude of 3 V and frequency of 150 kHz. The typical VPFM images are shown in Figure 4.

The sample in Figure 4a was solvent vapor annealed at 30 °C for 4 h. Before the VPFM measurement, the central area of 6 × 6 μm was first scanned with a sample bias of −10 V, and then the smaller central area of 4 × 4 μm was scanned with bias of +10 V. Finally, VPFM was performed at the central area of 8 × 8 μm. The height image in Figure 4a shows large aggregations, indicating the controlling of solvent vapor on film morphology. As for the VPFM phase image, in the central areas of 4 × 4 μm and 6 × 6 μm, image shows some blurry contours with contrary contrast, seemingly implying the reversed polarization states caused by ±10 V bias. However, the VPFM phase signals are so weak that it is hard to distinguish among positively and negatively polarized and even unpolarized areas. The VPFM

amplitude image also shows a very blurry contrast, indicating very weak piezoelectric signals detected by the AFM probe.

However, as for the film SVA treated for 6 h, we do observe obvious VPFM signals, as shown in Figure 4b. The height image shows similar small crystalline grains as those shown in Figure 1c. Before the VPFM measurement, the central area of 6 × 6 μm was first scanned with sample bias of −10 V, and then the lower half region of 6 × 3 μm in this negatively prepolarized area was scanned with a sample bias of +10 V. Finally, VPFM was performed within an 8 × 8 μm area. The VPFM phase image shows contrary contrast in the central area of 6 × 6 μm, which corresponds to reversed polarization states caused by the application of ±10 V bias. The phase signals in the central area are obviously different from those in the surrounding, also indicating the existence of both polarization states. The averaged phase difference between the positive and the negative polarization states is about 178°, well consistent with the expected value of 180°.<sup>18</sup> The VPFM amplitude image shows very obvious vibration signals in the central 6 × 6 μm area, indicating that, no matter if the central area is positively or negatively polarized, both polarization states exhibit good piezoelectricity. The averaged VPFM amplitude difference between the polarized and unpolarized states is about 1.4 mV.

Compared to the film SVA-treated for 6 h, the film SVA-treated for 4 h shows very weak ferroelectric and piezoelectric properties from the VPFM measurements in Figures 4a and 5b. This can be attributed to the relatively thinner crystalline layer in 4 h treated film. Due to short SVA time, solvent vapor can only diffuse a shallow level into the film, resulting in the crystallization only in the region adjacent to the film surface.

For comparison, we also conducted VPFM measurements on both as-coated and thermally annealed P(VDF-TrFE) thin films. The process for both VPFM measurements is the same as that for the 4 h treated film. Before the VPFM measurements, the central area of 6 × 6 μm was first scanned with −10 V sample bias, and then the smaller central area of 4 × 4 μm was polarized with a +10 V bias. Finally, VPFM was performed at the central area of 8 × 8 μm. After these polarization treatments, the as-coated P(VDF-TrFE) film still showed no observable ferroelectric and piezoelectric properties, as can be seen in Figure 4c. Note that the stripes in height image are due to the large mechanical interaction between the tip and the film surface, which results in the accumulation of the film. Both VPFM phase and amplitude images show no observable responses to VPFM driving voltage, which indicates that, for an as-coated film, the poling process cannot induce ferroelectric



and piezoelectric properties, even on a microscopic scale. As for the thermally annealed film, crystalline grains cover the whole film surface in the height images in Figure 4d, which implies the improvement of film crystallinity via thermal annealing. In the VPFM phase image, we get obvious phase separation with phase difference of about  $170^\circ$  between the positive and negative polarization states. VPFM amplitude image also indicates large piezoelectric property in both positive and negative polarization states, both of which are well distinguished from the surrounding unpolarized state. The averaged amplitude difference between the polarized and unpolarized states is about 2.2 mV, a little larger than that of  $\sim 1.4$  mV from the SVA-treated film shown in Figure 4b.

From all these VPFM measurements, we can find that although SVA treatment enhances the crystallinity and thus the ferroelectric and piezoelectric properties, the thermally annealed film still shows a better piezoelectric property. This may be due to the much thinner crystalline layer induced by the solvent vapor annealing. Further work should be done to improve the penetration of the solvent into film, such as selection of the suitable solvent, optimization of the environmental temperature and exposure time.

To illuminate the feasibility of low-temperature fabrication of ferroelectric devices via solvent vapor annealing, we further constructed Si-based ferroelectric capacitor memory devices with Al/P(VDF-TrFE)/Al<sub>2</sub>O<sub>3</sub>/p-Si/Al (MFeOS) structure, as shown in the inset of Figure 5. The fabrication process and structural parameters of such devices are well expounded in the Experimental Section. The P(VDF-TrFE) film was solvent vapor annealed at 30 °C for 6 h. The bistable operation of the MFeOS capacitors is evident in capacitance–voltage (*C*–*V*) measurements in Figure 5a. The capacitance shows clear hysteresis due to the bistable polarization states of the SVA-treated P(VDF-TrFE) film. Memory window width slightly increases from 1.06 to 1.59 V with an increase of gate voltage, *V<sub>g</sub>*, from 10 to 20 V. We designate “ON” as the state obtained after poling by large negative gate voltage, and “OFF” as the state after poling by large positive voltage. The capacitance ratio of the ON to the OFF states (ON/OFF ratio) is 2.8 at a *V<sub>g</sub>* of 0 V and reaches its maximum value of 3.6 at a *V<sub>g</sub>* of  $-0.6$  V. These ON/OFF ratios are comparable to, but a little smaller than those obtained from other MFeOS structures where ferroelectric P(VDF-TrFE) layers were thermally annealed.<sup>19,20</sup>

Typical retention performance of such MFeOS capacitors is shown in Figure 5b. Before retention measurements, a gate voltage of +20 V (–20 V) was applied for 10 s to drive the MFeOS capacitor into the OFF (ON) state. Then retention measurements were performed for 4000 s. Both ON and OFF states degrade with the increase of retention time and the capacitance difference between both states gradually decreases from 120 to 39.2 pF in 4000 s. The bad retention performance is usually attributed to depolarization in the ferroelectric layer.<sup>21</sup> Note that the fabrication process and structural parameters for our MFeOS capacitors are not optimized. After device structure optimization, it is expected to obtain an even better memory performance, such as a larger ON/OFF ratio, wider memory window and longer retention.

## CONCLUSION

In conclusion, we fabricated ferroelectric P(VDF-TrFE) thin films via solvent vapor annealing at low temperatures, which satisfied the requirement of a low temperature process in flexible ferroelectric devices. Structural and phase information

and electrical properties of P(VDF-TrFE) films with various SVA times were characterized and the results indicated that by solvent vapor annealing for appropriate times, such as 4–6 h here, it was possible to fabricate P(VDF-TrFE) films with both proper ferroelectricity and defect-free surfaces. We structured MFeOS capacitors where ferroelectric layers were solvent vapor annealed. The MFeOS capacitors showed obvious bistable operation, indicating the feasibility of a low-temperature process for ferroelectric devices by solvent vapor annealing.

## EXPERIMENTAL SECTION

**Sample Preparation.** Ferroelectric films were prepared by a spin-coating technique from a 1.0% by weight solution of 60/40 P(VDF-TrFE) in methyl ethyl ketone (MEK) onto well cleaned glass slides (for AFM morphology, SEM and XRD measurements) or Al predeposited glass substrates (for electrical measurements of VPFM and macroscopic ferroelectric switching). Then the as-coated films were SVA treated for various times. For those samples used for macroscopic ferroelectric switching measurements, after solvent vapor annealing, the top Al electrodes were vacuum deposited to form the Al/P(VDF-TrFE)/Al structure with an effective electrode area of 0.02 mm<sup>2</sup>. For comparison, some as-coated P(VDF-TrFE) samples were thermally annealed at 135 °C for 3 h to increase their crystallinity, the structure of which is analyzed and compared with those treated by the SVA method. The thickness of the SVA-treated and thermally annealed ferroelectric films was about 150 nm, which was determined by SEM (XL30FEG, PHILIPS, The Netherlands).

**Solvent Vapor Annealing.** A sealed glass cylinder container was filled with about 15 mL of MEK solvent and then kept at 30 °C for 1 h before SVA treatment. Then the as-coated P(VDF-TrFE) films were put into this sealed container with a separation of 5.0 mm from the surface of the MEK solvent. The container with P(VDF-TrFE) films stayed at 30 °C for a preset time and then the samples were taken out to perform further characterizations.

**Fabrication of Ferroelectric Capacitor Memory Devices.** Si-based ferroelectric capacitor memory devices were fabricated with the Al/P(VDF-TrFE)/Al<sub>2</sub>O<sub>3</sub>/p-Si/Al structure. The substrate was device level *p*-type Si(001) with a resistivity of 8–12 Ω cm. After a standard RCA cleaning, Si substrates were dipped in a diluted HF solution, followed by a DI water rinse and spin-drying process. A 5 nm thick Al<sub>2</sub>O<sub>3</sub> layer was deposited onto cleaned Si substrates by atomic layer deposition. The P(VDF-TrFE) layer was spin-coated from a 1.0% by weight solution onto Al<sub>2</sub>O<sub>3</sub>/p-Si substrates and then solvent vapor annealed at 30 °C for 6 h. Circular Al top gate electrodes with a thickness of 200 nm and diameter of 1.0 mm were deposited by vacuum evaporation through a shadow mask. Ohmic contact was made to the backside of the silicon with a vacuum-evaporated Al film of 200 nm thickness.

**Structural Characterizations.** Films deposited directly on glass substrates were used for structural characterizations. AFM (Nanoscope V, Bruker, Germany) in tapping mode was used to determine the morphologies of P(VDF-TrFE) films treated by both SVA and thermal annealing. XRD (D8, Bruker-AXS, Germany) was performed to determine the crystalline phase in P(VDF-TrFE) films.

**Electrical Measurements.** Films spin-coated on Al predeposited glass substrates were used for electrical measurements. Ferroelectric switching measurements were performed on Al/P(VDF-TrFE)/Al sandwich structures by a homemade Sawyer-Tower circuit. Polarization–voltage (*P*–*V*) hysteresis loops were obtained by integrating the recorded switching current with time. Nanoscale ferroelectric measurements on the P(VDF-TrFE)/bottom Al electrode structure were performed by vertical piezoresponse force microscopy (VPFM, Nanoscope V, Bruker, Germany) working in contact mode with driving amplitude of 3 V and frequency of 150 kHz. During the VPFM measurements, the conductive AFM probe was always electrically grounded and the voltage was applied to the bottom Al electrode. For electrical measurements of Al/P(VDF-TrFE)/Al<sub>2</sub>O<sub>3</sub>/p-Si/Al capacitors, the backside electrode was always grounded, while the voltage

was applied to the gate. Capacitance measurements were performed at exciting frequency of 1 MHz and amplitude of 50 mV by an Agilent 4294A Precision Impedance Analyzer.

## AUTHOR INFORMATION

### Corresponding Authors

\*S. Ding. E-mail: sjding@fudan.edu.cn.

\*G. Zhu. E-Mail: gdzhu@fudan.edu.cn.

### Notes

The authors declare no competing financial interest.

## ACKNOWLEDGMENTS

The authors thank the support from National Key Technologies R&D Program (2009ZX02302-002), National Natural Science Foundation of China (61076076, 61076068), STCSM (13NM1400600), NSAF(U1430106) and ZhuoXue Plan of Fudan University.

## REFERENCES

- (1) Hu, Z.; Tian, M.; Nysten, B.; Jonas, A. Regular Arrays of Highly Ordered Ferroelectric Polymer Nanostructures for Non-volatile Low-Voltage Memories. *Nat. Mater.* **2009**, *8*, 62–67.
- (2) Naber, R.; Asadi, K.; Blom, P.; Leeuw, D.; Boer, B. Organic Nonvolatile Memory Devices Based on Ferroelectricity. *Adv. Mater.* **2010**, *22*, 933–945.
- (3) Mao, D.; QuevedoLopez, M. A.; Stiegler, H.; Gnade, B. E.; Alshareef, H. N. Optimization of Poly(vinylidene fluoride-trifluoroethylene) Films as Non-volatile Memory for Flexible Electronics. *Org. Electron.* **2010**, *11*, 925–932.
- (4) Khim, D.; Baeg, K.; Kim, J.; Kang, M.; Lee, S.; Chen, Z.; Facchetti, A.; Kim, D.; Noh, Y. High Performance and Stable N-Channel Organic Field-Effect Transistors by Patterned Solvent-Vapor Annealing. *ACS Appl. Mater. Interfaces* **2013**, *5*, 10745–10752.
- (5) Luca, G.; Liscio, A.; Nolde, F.; Scolaro, L. M.; Palermo, V.; Müllen, K.; Samori, P. Self-Assembly of Discotic Molecules into Mesoscopic Crystals by Solvent-Vapour Annealing. *Soft Matter* **2008**, *4*, 2064–2070.
- (6) Ludwigs, S.; Böker, A.; Voronov, A.; Rehse, N.; Magerle, R.; Krausch, G. Self-Assembly of Functional Nanostructures from ABC Triblock Copolymers. *Nat. Mater.* **2003**, *2*, 744–747.
- (7) Sinturel, C.; Bayer, M.; Morris, M.; Hillmyer, M. A. Solvent Vapor Annealing of Block Polymer Thin Films. *Macromolecules* **2013**, *46*, 5399–5415.
- (8) Balakrishnan, K.; Datar, A.; Naddo, T.; Huang, J.; Oitker, R.; Yen, M.; Zhao, J.; Zang, L. Effect of Side-Chain Substituents on Self-Assembly of Perylene Diimide Molecules: Morphology Control. *J. Am. Chem. Soc.* **2006**, *128*, 7390–7398.
- (9) Wang, H.; Liu, J.; Xu, Y.; Han, Y. Fibrillar Morphology of Derivatives of Poly(3-alkylthiophene)s by Solvent Vapor Annealing: Effects of Conformational Transition and Conjugate Length. *J. Phys. Chem. B* **2013**, *117*, 5996–6006.
- (10) Khan, H. U. Solvent Vapor Annealing in the Molecular Regime Drastically Improves Carrier Transport in Small-Molecule Thin-Film Transistors. *ACS Appl. Mater. Interfaces* **2013**, *5*, 2325–2330.
- (11) Chen, H.; Hsiao, Y.; Hu, B.; Dadmun, M. Control of Morphology and Function of Low Band Gap Polymer–bis-Fullerene Mixed Heterojunctions in Organic Photovoltaics with Selective Solvent Vapor Annealing. *J. Mater. Chem. A* **2014**, *2*, 9883–9890.
- (12) Wessendorf, C.; Schulz, G.; Mishra, A.; Kar, P.; Ata, I.; Weidener, M.; Urdanpilleta, M.; Hanisch, J.; Mena-Osteritz, E.; Lindén, M.; Ahlswede, E.; P. Bäuerle, P. Efficiency Improvement of Solution-Processed Dithienopyrrole-based A-D-A Oligothiophene Bulk-Heterojunction Solar Cells by Solvent Vapor Annealing. *Adv. Energy Mater.* **2014**, *4*, 1–10. DOI: 10.1002/aenm.201400266.
- (13) De Gennes, P. G. Wetting: Statics and Dynamics. *Rev. Mod. Phys.* **1985**, *57*, 827–863.
- (14) De Luca, G.; Treossi, E.; Liscio, A.; Mativetsky, J. M.; Scolaro, L. M.; Palermo, V.; Samori, P. Solvent Vapour Annealing of Organic Thin Films: Controlling the Self-Assembly of Functional Systems Across Multiple Length Scales. *J. Mater. Chem.* **2010**, *20*, 2493–2498.
- (15) aDicksens, B.; Balizer, E.; DeReggi, A.; Roth, S. Hysteresis Measurements of Remanent Polarization and Coercive Field in Polymers. *J. Appl. Phys.* **1992**, *72*, 4258–4264.
- (16) Noda, K.; Ishida, K.; Kubono, A.; Horiuchi, T.; Yamada, H.; Matsushige, K. Remanent Polarization of Evaporated Films of Vinylidene Fluoride Oligomers. *J. Appl. Phys.* **2003**, *93*, 2866–2870.
- (17) Wang, F.; Lack, A.; Xie, Z.; Fröbing, P.; Taubert, A.; Gerhard, R. Ionic-Liquid-Induced Ferroelectric Polarization in Poly(vinylidene fluoride) Thin Films. *Appl. Phys. Lett.* **2012**, *100*, 062903-1–062903-4.
- (18) Kalinin, S. V.; Rar, A.; Jesse, S. A Decade of Piezoresponse Force Microscopy: Progress, Challenges, and Opportunities. *IEEE Trans. Ultrason. Ferroelectr. Freq. Control* **2006**, *53*, 2226–2252.
- (19) Fujisaki, S.; Ishiwara, H.; Fujisaki, Y. Low-Voltage Operation of Ferroelectric Poly(Vinylidene Fluoridetrifluoroethylene) Copolymer Capacitors and Metal-Ferroelectric-Insulator-Semiconductor Diodes. *Appl. Phys. Lett.* **2007**, *90*, 162902-1–162902-3.
- (20) Müller, K.; Henkel, K.; Mandal, D.; Seime, B.; Paloumpa, I.; Schmeißer, D. Spin-coated Organic Ferroelectric Films for Non-volatile Memories. *Phys. Status Solidi A* **2011**, *208*, 330–342.
- (21) Ma, T. P.; Han, J. Why is Nonvolatile Ferroelectric Memory Field-Effect Transistor Still Elusive? *IEEE Electron. Device Lett.* **2002**, *23*, 386–388.